Journal of
Materials Chemistry C

Accepted Manuscript

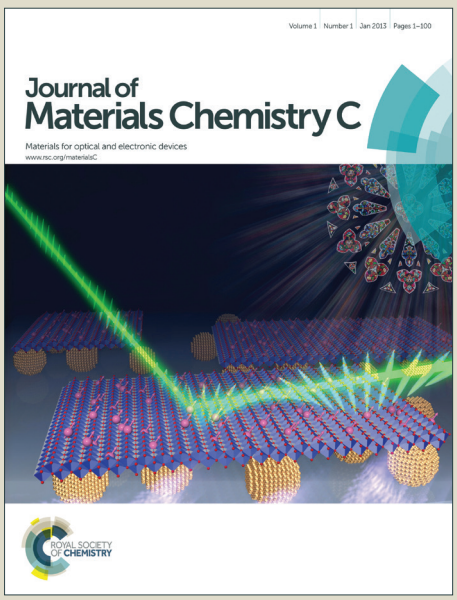

This is an *Accepted Manuscript*, which has been through the Royal Society of Chemistry peer review process and has been accepted for publication.

Accepted Manuscripts are published online shortly after acceptance, before technical editing, formatting and proof reading. Using this free service, authors can make their results available to the community, in citable form, before we publish the edited article. We will replace this *Accepted Manuscript* with the edited and formatted *Advance Article* as soon as it is available.

You can find more information about *Accepted Manuscripts* in the Information for Authors.

Please note that technical editing may introduce minor changes to the text and/or graphics, which may alter content. The journal's standard Terms & Conditions and the Ethical guidelines still apply. In no event shall the Royal Society of Chemistry be held responsible for any errors or omissions in this *Accepted Manuscript* or any consequences arising from the use of any information it contains.

ROYAL SOCIETY OF CHEMISTRY

www.rsc.org/materialsC

Solvent-dependent self-assembly and ordering in slow-drying drop-cast conjugated polymer films

Kui Zhao,[ab] Xinhong Yu,[b] Ruipeng Li,[c] Aram Amassian[c] and Yanchun Han[b]**

[a]*School of Materials Science and Engineering, Shaanxi Normal University, Xian 710119, People's Republic of China.*

[b]*State Key Laboratory of Polymer Physics and Chemistry, Changchun Institute of Applied Chemistry, Chinese Academy of Sciences, 5625 Renmin Street, Changchun 130022, People's Republic of China.*

[c]*Materials Science and Engineering, Division of Physical Sciences and Engineering, Solar and Photovoltaic Engineering Research Center, King Abdullah University of Science and Technology (KAUST), Thuwal, Saudi Arabia.*

Email: kuizhao918@foxmail.com. ychan@ciac.jl.cn

Abstract:

The mechanistic understanding of the intrinsic molecular self-assembly of conjugated polymers is of immense importance to controlling the microstructure development in organic semiconducting thin films, with meaningful impact on charge transport and optoelectronic properties. Yet, to date the vast majority of studies have focused on the fast solution process itself, with studies of slower intrinsic molecular self-assembly in formulations lagging behind. Here we have investigated molecular self-assembly during spontaneous organization and uncovered how changes in formulation influence the microstructure, morphology and transport properties of conjugated polymer thin films. Our results suggest that the polymer-solvent interaction is the key factor for the molecular self-assembly and changes in macroscopic charge transport, which is in contrast with most solution processes, such as spin-coating and blade coating, where solvent drying kinetics dominates the

Journal of Materials Chemistry C Accepted Manuscript

aggregation and crystallization processes. Energetically favourable interactions between the polymer and its solvent are shown to cause chain expansion, resulting in a large hydrodynamic volume and few chain entanglements in solution. This provides molecular freedom for self-assembly and is shown to greatly enhance the local and long range order of the polymer, intra-chain backbone planarity and crystallite size. These improvements, in turn, are shown to endow the conjugated polymer with high carrier transport, as demonstrated by organic thin film transistors.

Introduction

The ordering and crystallization of semicrystalline conjugated polymers, such as poly(3-hexylthiophene) (P3HT), mediates their optical, electronic and transport properties in the solid state.[1,2] The alkyl side chains determine the solubility of the polymer and its stacking, resulting in a rigid conjugated backbone contributing to π-π stacking and in some cases to the formation of one-dimensional (1-D) crystalline nanofibrils.[3-6] Polymer crystallization from solution is a complex exothermic process.[7] For example, the nucleation process is determined by solvent-polymer interactions which drive conformational transition to form planar lamellae. The growth process is mostly determined by molecular diffusion, entanglement effect, de/formation process and as such.[7] As polymer crystallization behavior is a key parameter determining molecular stacking order and microstructure in solid thin films with significant consequences for charge transport,[3,4,8] different approaches have been adopted to control the molecular self-assembly and microstructure of P3HT thin films, including decreasing chain entanglements in the solution state,[9,10] tuning solution-processing conditions,[11-14] and applying post-thermal or solvent annealing.[15-17]

Journal of Materials Chemistry C Accepted Manuscript

Despite progress in controlling aggregation in solution, coating processes such as spin-coating remain by far the most common method for materials screening and device optimization.[18] This is not surprising as spin-coating is a simple and rapid method which produces uniform films on small substrates with the desired thickness and uniform layer.[19] However spin-casting induces rapid solvent evaporation which can kinetically quench the self-assembly processes that require longer time scale.[20] The microstructure in such thin films therefore tends to be highly dependent upon other dynamical factors, including drying kinetics, rather than the intrinsic molecular interactions.[21-23] For instance, a poor solvent having lower volatility than the main solvent of a formulation is likely to reside for a longer duration in the drying film, thus promoting the nucleation and growth of ordered aggregates as the formulation transitions from a mixture of solvents to a marginal solvent.[21] A highly volatile solvent can also lead to enhanced supramolecular assembly if it interacts with the main solvent through hydrogen bonding.[23] The key requirement to obtaining high local and long range order in polymer thin films is sufficient time to undergo self-assembly. As such, drop-casting a solution in a closed container can provide sufficient time for molecular self-assembly to organize the polymer film.[24] Unfortunately, there are very few reports looking at how solution formulation tunes the intrinsic molecular interactions in conjugated polymers and changes the microstructure and morphology of polymer thin films, let alone the transport properties of the semiconductor.

Herein, we show that the long time self-assembly of conjugated polymer can be strongly influenced by the solution formulation. The thin film formation occurs very slowly in a closed container with extremely slow solvent evaporation. We have investigated the solution state of the polymer using UV-Vis absorption and dynamical light scattering (DLS) and characterised the dry thin films by x-ray diffraction, grazing incidence wide-angle X-ray scattering (GIWAXS),

Journal of Materials Chemistry C Accepted Manuscript

transmission electron microscopy (TEM) and UV-Vis absorption with quantitative analysis using the Spano method. Our analysis suggests that small but energetically favourable interactions between the polymer and the solvent can promote local and long range order of the semi-crystalline conjugated polymer [poly-3(hexylthiophene) (P3HT)] and tune the formation of morphological features, such as ribbons and fibrils, with significant implications on carrier transport in organic thin film transistors (OTFTs).

Results and discussion

1. Solvent-polymer interaction

Four solvents, CS_2, CB, $CHCl_3$ and toluene were used to endow different self-assembly characteristics to the solution formulation. The Hansen solubility parameters ($\Delta\delta$) of the polymer and solvents,[25,26] as well as other relevant parameters are summarized in **Table 1**. Comparing the total Hansen solubility parameters of P3HT with that of solvents at room temperature reveals toluene to be the poorest solvent, followed by $CHCl_3$, while CB and CS_2 are much better solvents for P3HT.[6,27,28,29] Based on this, toluene is more likely to behave as a theta solvent at room temperature, in agreement with previous observations.[10] The intermolecular interactions between polymer chain segments and coordinated solvent molecules have an associated energy of interaction which can be positive or negative. For a good solvent, e.g. CS_2, interactions between polymer segments and solvent molecules are energetically favourable, which causes expansion of polymer coils which results in a larger hydrodynamic volume and negligible chain entanglements.[30] In a poor solvent, such as toluene, polymer-polymer interactions are preferred, and the polymer coils will contract, causing aggregation and possibly micro-crystallite formation as well as chain entanglements in

Journal of Materials Chemistry C Accepted Manuscript

solution. This is confirmed by probing the optical properties of the polymer solution. The UV-Vis absorption spectra show a clear peak at ca. 605 nm for P3HT in toluene, which is associated to inter-chain interactions in nucleates/micro-crystallites (**Figure 1a**),[31,32] while no such peak is present for the other solvents. The status of polymer chains in solution was further investigated by dynamic light scattering (DLS) and rheometer (**Figure 1b**, see **Figure S1** for more details). The z-average size of P3HT aggregates increases from ~28 nm in CS_2 to ~98 nm in toluene, strongly suggesting that the polymer chains contract and aggregate in the latter theta solvent in comparison to good solvent.[30] We observe an increase of the viscosity of the solution from 0.26 cp to 0.59 cp when changing from CS_2 to the theta solvent at the same concentration. The higher viscosity of the toluene-based solution indicates stronger intermolecular interactions and chain entanglements.[33]

Table 1. The Hansen solubility parameters of those four solvents and P3HT as well as other parameters of four different solvents at room temperature.

	CS_2	CB	$CHCl_3$	toluene	P3HT
T_b (°C)	40	132	61	111	–
$\delta_D(cal\cdot cm^{-3})^{1/2}$	10	9.29	8.70	8.80	9.02
$\delta_P(cal\cdot cm^{-3})^{1/2}$	0	2.10	1.52	0.68	2.58
$\delta_H(cal\cdot cm^{-3})^{1/2}$	0.30	0.98	2.79	0.98	2.58
$\delta_T(cal\cdot cm^{-3})^{1/2}$	10	9.57	9.29	8.88	9.75
$\lvert\Delta\delta_T\rvert = \lvert\delta_{P3HT} - \delta_{solvent}\rvert$	0.25	0.18	0.46	0.87	–
Dipole moment (D)	0	1.54	1.15	0.36	–

Journal of Materials Chemistry C Accepted Manuscript

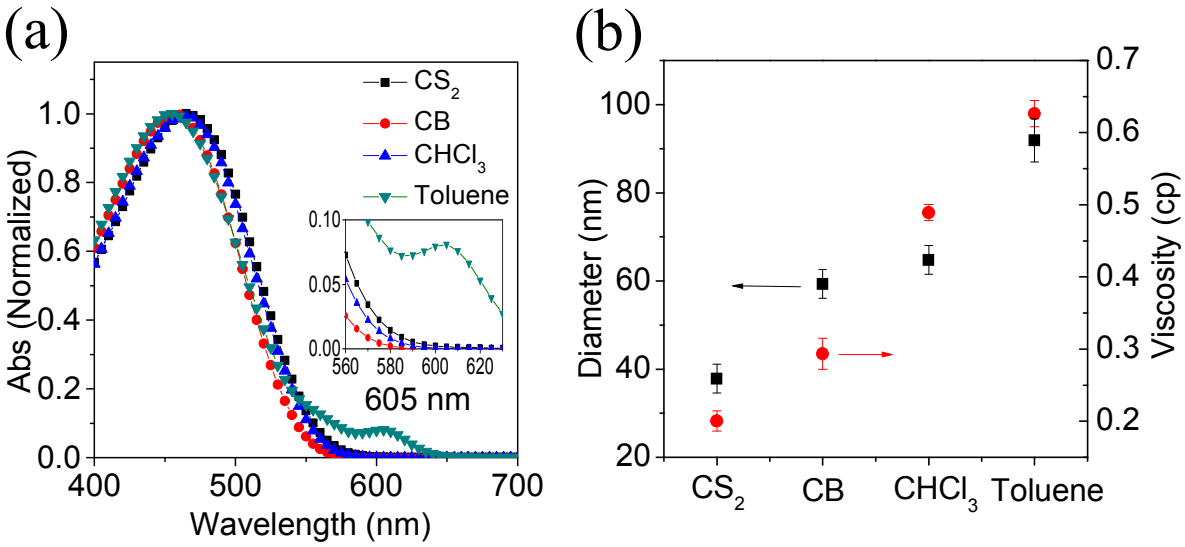

Figure 1. (a) UV-vis absorption of P3HT solutions (0.01 wt%) with various solvents. (b) Dynamical light scattering (DLS) and rheometer of P3HT in different solvents showing differences in the Z-average size of P3HT particles and viscosity of the solutions.

To allow the solvent-polymer interactions to play out, we performed solution-casting in a sealed container, as shown in **Figure 2a**. The solvents thus dry much more slowly than normally, e.g., 20 min for the CS_2 solution (instead of ~10 sec in open space) and over 20 hours for CB solution (instead of ~5 min), respectively (**Figure 2b**). As such, the slow evaporation of solvents in an enclosed space provides a high solvent vapor pressure which acts similarly as solvent vapor annealing. By contrast, solutions dry in a matter of seconds by spin-casting.[34,35]

Journal of Materials Chemistry C Accepted Manuscript

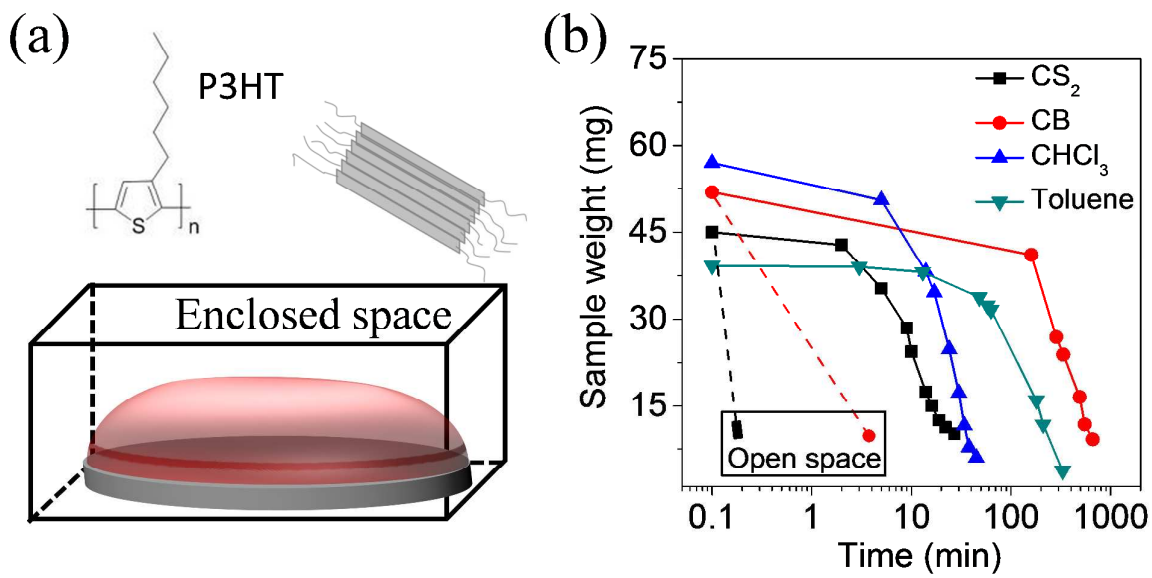

Figure 2. (a) Solution-casting performed in an enclosed space, giving rise to extremely slow evaporation of solvents for efficient self-assembly. (b) Solvents drying kinetics for P3HT solutions in an enclosed space and an open space.

2. Device performance

The field-effect mobility in P3HT thin films was measured by fabricating bottom-gate top-contact (BGTC) OTFTs (**Figure 3a**, inset). The average saturation hole mobility is plotted in **Figure 3a** (see **Figure S2** for more details). The device prepared from slow-casting the toluene solution achieves an average mobility of 0.002 cm^2/Vs and I_{on}/I_{off} ~360. These results are similar to the performance of spin-cast films from the same solvent toluene,[10,33] indicating little or no benefit of slow casting when using toluene. The average mobilities of devices increase gradually by more than an order of magnitude to 0.028 cm^2/Vs when changing the solvent from toluene to $CHCl_3$, CB and finally CS_2. The I_{on}/I_{off} increases 20-fold as well, topping up at ~10^4 (**Figure S2a**). These results indicate a strong dependence of the carrier mobility in P3HT films slow-cast in the presence of

Journal of Materials Chemistry C Accepted Manuscript

different polymer-solvent interactions, with the more favourable interactions leading to higher carrier mobility, as seen in **Figure 3b**. It is well established that carrier transport in high Mw semicrystalline polymers, such as P3HT, proceeds through ordered regions and hops between these ordered regions through tie chains.[36] Hence, our results suggest that polymer-solvent interactions have a strong and meaningful impact on microstructural and morphological aspects which mediate charge transport.

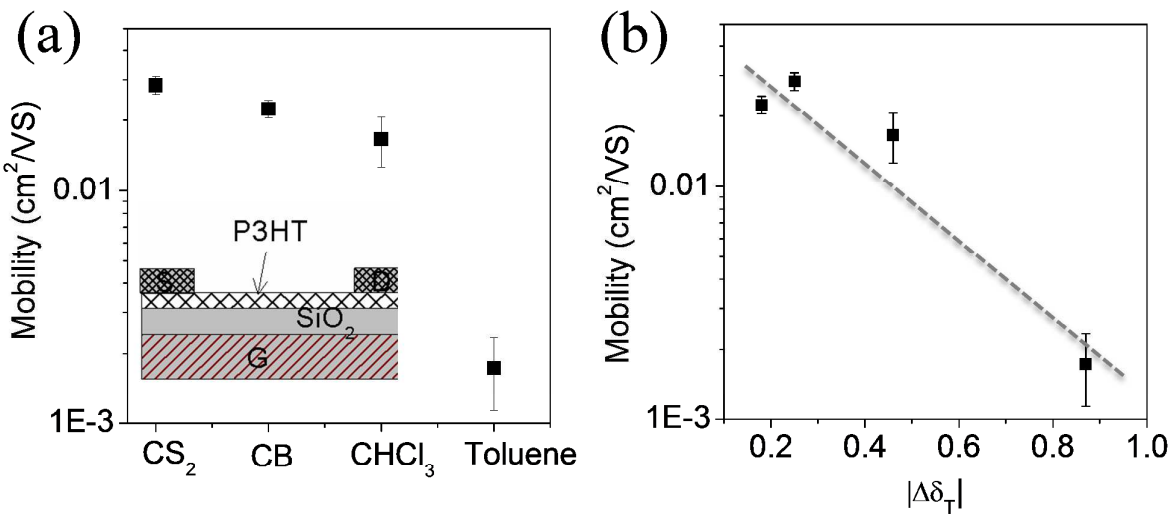

Figure 3. Electrical characteristics in ambient conditions of a representative OTFT for thin films from various solvents. (a) Field-effect mobility; (b) Field-effect mobility *vs.* polymer-solvent interaction.

3. Mesoscale morphology and molecular order

In **Figure 4** we compare the mesoscale morphology of the slow-cast films observed by optical microscopy and transmission electron microscopy (TEM). The films prepared by slow-casting exhibit widely different mesoscale morphologies, some of which are visible optically. The CS_2-cast film shows very well-developed microscale ribbons, with tens of micrometres in length and up to micrometers in width. These features are very different from fibrillar features typically attributed to

Journal of Materials Chemistry C Accepted Manuscript

P3HT cast from theta solvents, and which is observed in the case of films cast from toluene.[10] We could not find any signature of ribbon formation from any other solvents investigated herein. The densely stacked ribbons observed in CS_2-cast films represent a typical superstructure of polymer lamellae. The formation of densely packed long ribbons without distinct grain boundaries is partially attributed to below factors. The energetically favorable polymer-solvent interaction causes chain expansion to result in few chain entanglements and provides sufficient molecular freedom for P3HT self-assembly into ribbons. This is aided by the slow evaporation of CS_2 in the closed container, which provides sufficient time for ribbon formation. With the removal of entanglements, we believe that nucleation density is reduced and instead crystallization and growth are promoted by virtue of molecular incorporation into the microscale ribbons. The other solvents yielded fibril formation, with lateral length scale varying strongly with choice of solvent. In the cases of CB, $CHCl_3$ and toluene solvents, the fibrils were short and randomly distributed, with length of several micrometers, which is more similar to the reported observation of spin-cast films.[17]

It should be noted that both ribbons and fibrils show a well-developed interconnection between grains in thin films, due to the existing tie molecules of high Mw P3HT linking ordered domains.[10] Charge transport in polymer OTFTs is determined by the slowest process. Transport within the domains is assured by a combination of intra-chain and inter-chain processes, whereas transport between domains relies on a combination of domain boundary hopping and the presence or not of tie molecules linking ordered domains. The observation of well-developed interconnection makes it possible that domain boundary hopping does not appear to be a critical process in these four films; whilst the device performance is more likely determined by charge transport within domains.

Journal of Materials Chemistry C Accepted Manuscript

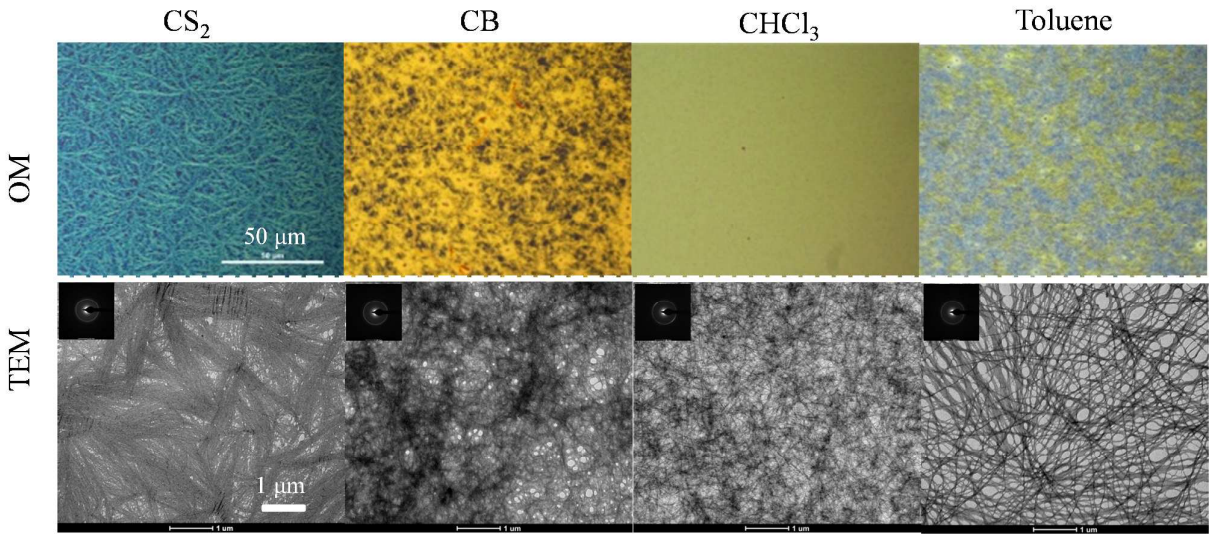

Figure 4. Optical microscopy (OM) and transmission electron micrographs (TEM) for P3HT thin-films cast from various solvents. Inset showing the corresponding selected area electron diffraction (ED) of TEM images.

We further investigate the P3HT aggregation behavior quantitatively to assess how local and long range order is influenced by the polymer-solvent interactions. Correcting for film thickness, the (100) out-of-plane lamellar X-ray diffraction (XRD) intensity suggests decreasing lamellar texture or order going from CS_2 to CB, to $CHCl_3$ and finally toluene (**Figure 5a**). The lamellar diffraction intensity of the CS_2-cast film is 3 times higher than the sample cast from toluene, which is most likely due to differences in the degree of crystalline ordering in the lamellar direction. The drying time was previously reported as a key factor affecting the microcrystalline development by static and time-resolved studies.[22,35,37] However, our analysis indicates that these improvements in the long range order during slow-casting from various solvents is more closely determined by the polymer-solvent interactions than the drying process.

Journal of Materials Chemistry C Accepted Manuscript

The full width half maximum (FWHM) of the azimuthal-angle intensity of the GIWAXS q_z= (100) Bragg sheet, was calculated to investigate the lamellar texture and mosaicity (**Figure 5b**, see **Figure S3** for more details). The FWHM ranges from 14° to 11° for all solvents-cast samples, indicating highly oriented molecules with "edge-on" packing and negligible effect from solvent on anisotropic behavior. By contrast, we note that spin-coated films present more randomly orientational distribution of nanocrystallites, e.g., FWHM=20° for the toluene-cast sample.[10] This is most likely because of fast kinetically quenched chain packing during fast spinning process. The highly textured lamellae indicate a predominantly edge-on stacking configuration on the substrate, which should favor charge-carriers transport through π-π stacking.[38]

The spacings along the π- and lamellar stacking directions of P3HT crystallites were calculated from electron diffraction (ED) and XRD. It was found both spacings follow the order decreasing from CS_2 >CB> $CHCl_3$ ≥toluene (**Figure 5c**). The CS_2-cast film exhibits π-stacking spacing of ~0.40 nm and lamellar stacking spacing of ~1.8 nm, respectively 0.02 nm and 0.1 nm larger than the toluene-cast film, respectively. The decreased spacings when using the theta solvent is associated to more close packing of P3HT chains due to unfavorable interactions between the polymer and the solvent. However, close packing along the π-stacking direction does not imply larger or more correlated domains. The crystalline correlation length of P3HT along the lamellar direction was calculated from the (100) peak obtained in the XRD configuration using the Debye-Scherrer method and is plotted in **Figure 5d**.[39] The correlation length decreases from ca. 23 nm for CS_2-cast films to 16-18 nm for the other solvent-cast films, indicating the formation of more long range order in the lamellar stacking direction of P3HT when cast from a very good solvent. Surprisingly, the expansion along alkyl side chains and the broadening of π-π distance do not result in decrease in the

Journal of Materials Chemistry C Accepted Manuscript

charge-carriers mobility, similar to previous observations.[40] This proves that efficient pathways are present for charge-carrier transport despite the significant increase in the π-π stacking distance.

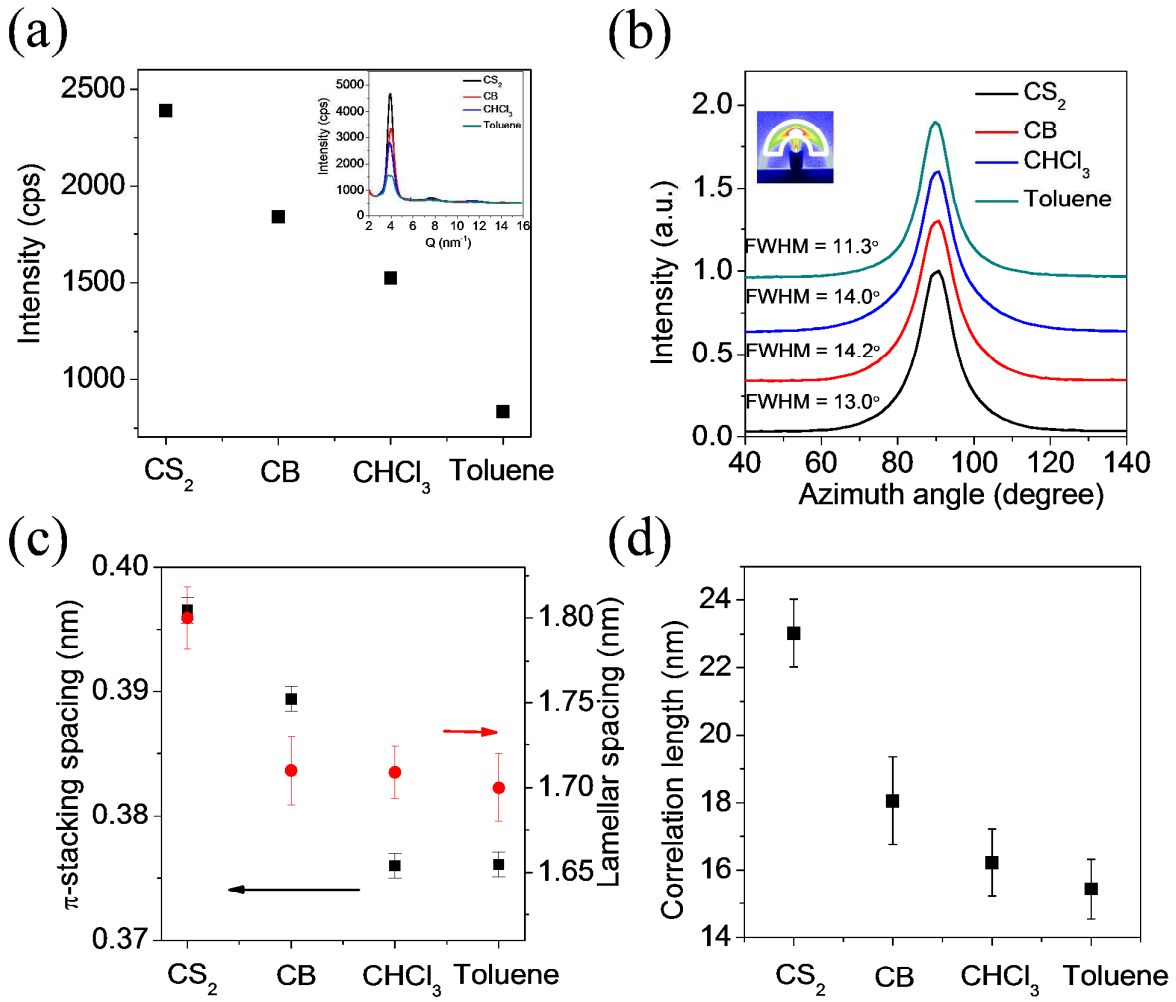

Figure 5. (a) The XRD out-of-plane (100) lamellar diffraction intensity of all P3HT thin-films. (b) The full width half maximum (FWHM) of the azimuthal-angle intensity of the GIWAXS q_z= (100) Bragg sheet. (c) The spacings along the π- and lamellar stacking directions of P3HT crystallites obtained from electron diffraction and XRD. (d) Correlation length of P3HT crystals calculated from (100) peak of XRD using Debye-Scherrer method.

Journal of Materials Chemistry C Accepted Manuscript

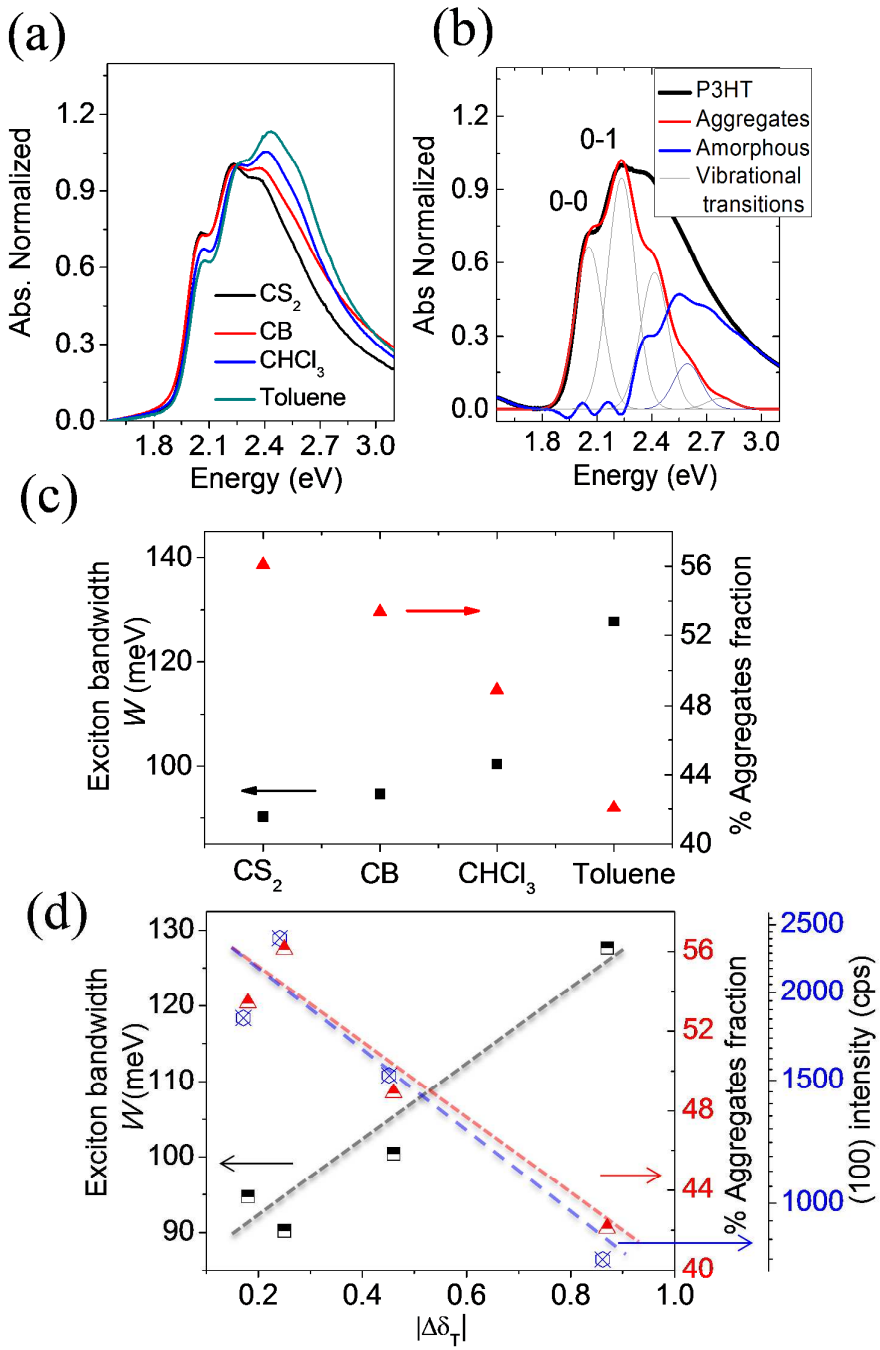

Figure 6. (a) UV-Vis absorption spectra of P3HT thin-films cast from various solvents. (b) Absorption spectrum of P3HT thin-film subjected to the Spano analysis. (c) The evolution of exciton bandwidth *W* (left axis) and fraction of film made up of aggregates (right). (d) The evolution of *W*, fraction of photo-aggregates and lamellar stacking intensity against polymer-solvent interactions.

Journal of Materials Chemistry C Accepted Manuscript

We now turn our attention to understanding how polymer-solvent interactions influence the local order within the polymer. The photophysical aggregation of the conjugated monomer units, both in terms of inter-chain and intra-chain interactions, can be analyzed by UV-Vis absorption. The absorption spectrum is composed of a lower energy contribution from photophysical aggregates and higher energy contributions from more disordered chains (**Figure 6a**). The spectra were modeled using the Spano model according to equation (1) below, which has been successfully implemented and described in detail elsewhere (**Figure 6b**):[1,10,22,41-43]

$$\mathrm{A}(E) \propto \sum_{m=0}\left(\frac{S^m}{m!}\right) \times \left(1 - \frac{We^{-s}}{2E_p}\sum_{\mathrm{n}\neq\mathrm{m}}\frac{S^n}{n!n-(m)}\right)^2 \times \exp\left(\frac{\left(E-E_{0-0}-\mathrm{m}E_p-{}^1/_2\,WS^m e^{-S}\right)^2}{2\sigma^2}\right) \qquad (1)$$

where A is the absorbance as a function of the photon energy (E), W is the free exciton bandwidth of the aggregates, S is the Huang-Rhys factor and fixed at 1.0 taken from a Franck-Condon fit, m and n are differing vibrational levels, $E_{0\text{-}0}$ is the 0-0 transition energy, E_p is the intermolecular vibrational energy and taken as 0.18 eV, and σ is the Gaussian linewidth.

Based on the Spano analysis, we have calculated the fraction of P3HT photophysical aggregates and the exciton bandwidth, W, which is inversely related to the exciton conjugation length (also known as intra-chain exciton coupling) along the backbone and its planarity. The fraction of P3HT photophysical aggregates throughout the film decreases from 56% to 42%, when going from CS_2 to toluene, indicating substantial loss of overall local order when slow-casting using a theta solvent. The exciton bandwidth W increases gradually from 90 to 127 meV when changing the solvent from CS_2 to toluene, indicating that favorable solvent-polymer interactions promote extended conjugation length and planarity of the P3HT backbone. These observations of local order along the backbone and in the π-stacking direction as well as the trend in substantially increased long range order in the

Journal of Materials Chemistry C Accepted Manuscript

lamellar stacking direction indicate that energetically favorable polymer-solvent interactions can substantially improve the molecular level as well as microscale order in semicrystalline conjugated polymers (**Figure 6d**). While it is true that exciton bandwidth is strongly dependent upon the solvent boiling point for fast drying processes, such as spin-coating,[22] where the solvent drying rate determines the degree of kinetic quenching, our investigation demonstrates quite conclusively that given sufficient exposure time, solvent-polymer interactions can favorably impact the local and long range order in the conjugated polymer in ways that traditional solution processing approaches do not allow. This also explains why solution-processed thin films often benefit from post-deposition thermal or solvent vapor annealing treatments for further development of local and long range order.[17,44] We believe that the higher hydrodynamic volume of chains and fewer chain entanglements resulting from using good solvents endow greater facility for high quality polymer self-assembly. On the other hand, marginal solvents such as toluene, energetically unfavourable interactions prematurely cause chain coiling and entanglements which can disrupt development of local and long range order.

4. Conclusion

We have investigated the influence of weak solvent-polymer interactions on the self-assembly and ordering of conjugated polymers using a slow-casting method. By doing away with the inherent drying rate of these solvents and allowing the interactions to dominate the self-assembly process, we strongly influence the development of local and long range order in polymer films with important consequences on charge carrier transport. Favorable polymer-solvent interactions are shown to lead to long range order more easily than theta solvents, which lead to smaller hydrodynamic volume and

Journal of Materials Chemistry C Accepted Manuscript

more entanglements. These observations are in contrast with most solution processes, such as spin-coating and blade coating, where solvent drying kinetics dominate the aggregation and crystallization processes and where drying kinetics plays a more important role in the development of local and long range order.

Acknowledgement

Part of this work was supported by the National Natural Science Foundation of China (21334006) and the Strategic Priority Research Program of the Chinese Academy of Sciences (Grant No. XDB12020300).

Experimental Section

Materials: The regioregular poly(3-hexyl thiophene) P3HT (98.5% regioregularity, Mw = 67 kDa, Sigma-Aldrich Co) was used as received. Solvents, such as toluene, carbon disulfide (CS_2), chlorobenzene (CB), and chloroform ($CHCl_3$) were purchased from Beijing Chemical Company, China (Solvent parameters are summarized in **Table 1**). The solvents were used without further purification. The glass cover slides and silicon wafers were cleaned in a piranha solution (70/30 v/v of concentrated H_2SO_4 and 30% H_2O_2) at 90°C for 20 min, then thoroughly rinsed with deionized water, and finally blown dry in nitrogen.

Sample Preparation and Characterization: P3HT homogeneous thin films were prepared by dropping 0.01 wt% solutions on a substrate placed inside a closed container in which the solvent evaporates very slowly. UV-Vis absorption spectra were acquired using a Cary 5000 (Varian) instrument and dynamic light scattering (DLS) measurements on solutions were carried out using

Journal of Materials Chemistry C Accepted Manuscript

Zetasizer Nano ZS system from Malvern Instruments Ltd at room temperature. Rheology measurements were carried out on an Anton Paar MCR-301 rheometer at a constant shear rate of (100 s^{-1}). Thin films were characterized by optical microscopy, and bright field transmission electron microscopy carried out using a FEI Tecnai 12 operated at 120 kV accelerating voltage. The film thickness was measured using spectroscopic ellipsometry (SE; M-2000XI, J. A. Woollam Co., Inc). Grazing incidence wide angle X-ray scattering (GIWAXS) was carried out at D-line at the Cornell High Energy Synchrotron Source (CHESS) at Cornell University. A 0.5 × 0.1 mm beam size with a wavelength of 1.23 Å and wide band pass (1.47%) was generated from double-bounce multilayer monochromator. The incident angle of the X-ray beam was at 0.15 degree and the integration time was 1s.

Device Fabrication and Characterization; highly doped n-type silicon wafers (100) with thermally evaporated 300 nm SiO_2 was used for bottom gate OTFTs fabrication. Gold source and drain electrodes were evaporated through a shadow mask with a channel width (*W)* of 500 μm and length *(L*) of 50 μm. All electrical measurements were performed with a Keithely 4200 Semiconductor Characterization System in ambient air.

References:

1 F. C. Spano and C. Silva, *Annu. Rev. Phys. Chem*. 2014. **65**, 477.

2 E. B. Pentzer, F. A. Bokel, R. C. Hayward and T. Emrick, *Adv. Mater*. 2012, **24**, 2254.

3 T. J. Prosa, M. J. Winokur, J. Moulton, P. Smith and A. J. Heeger, *Macromolecules* 1992, **25**, 4364.

Journal of Materials Chemistry C Accepted Manuscript

4 I. Mcculloch, M. Heeney, M. L. Chabinyc, D. Delongchamp, R. J. Kline, M. Coelle, W. Duffy, D. Fischer, D. Gundlach, B. Hamadani, R. Hamilton, L. Richter, A. Salleo, M. Shkunov, D. Sporrowe, S. Tierney and W. Zhong, *Adv. Mater.* 2009, **21**, 1091.

5 E. Mena-osteritz, A. Meyer, B. M. W. Langeveld, R. A. J. Janssen, E. W. Meijer and P. Bäuerle, *Angew. Chem. Int. Ed*. 2000, **39**, 2680.

6 W. B. Hu, D. Frenkel, *"Polymer Crystallization Driven by Anisotropic Interactions" Adv. Polym. Sci.* Springer-Verlag Berlin Heidelberg, 2005.

7 M. Muthukumar, "*Nucleation in polymer crystallization*" *Advances in Chemical Physics*, Vol 128, ISBN 0-471-44528-2.

8 H. N. Tsao and K. Müllen, *Chem. Soc. Rev.* 2010, **39**, 2372.

9 K. Zhao, L. Xue, J. Liu, X. Gao, S. Wu, Y. Han and Y. Geng, *Langmuir* 2010, **26**, 471.

10 K. Zhao, H. U. Khan, R. Li, Y. Su and A. Amassian, *Adv. Funct. Mater*. 2013, **23**, 6024.

11 M. Brinkmann and J.-C. Wittmann, *Adv. Mater*. 2006, **18**, 860.

12 A. Salleo, R. J. Kline, D. M. DeLongchamp and M. L. Chabinyc, *Adv. Mater*. 2010, **22**, 3812.

13 Y. Fu, C. Lin and F.-Y. Tsai, *Org. Electron*. 2009, **10**, 883.

14 N. Kiriy, E. Jahne, H.-J. Adler, M. Schneider, A. Kiriy, G. Gorodyska, S. Minko, D. Jehnichen, P. Simon, A. A. Fokin and M. Stamm, *Nano Lett*. 2003, **3**, 707.

15 I. Roy and S. Hazra, *RSC Adv*. 2015, **5**, 665.

16 X. Xiao, Z. Wang, Z. Hu and T. He, *J. Phys. Chem. B* 2010, **114***,* 7452.

17 C.-M. Fu, K.-S. Jeng, Y.-H. Li, Y.-C. Hsu, M.-H. Chi, W.-B. Jian and J.-T. Chen, *Macromol. Chem. Phys.* 2015, **216**, 59.

Journal of Materials Chemistry C Accepted Manuscript

18 S. Ludwigs, "*P3HT Revisited – from Molecular Scale to Solar Cell Devices*" Springer Heidelberg New York Dordrecht London, ISBN 978-3-662-45144-1.

19 N. Sah, B. Parija and S. Panigrahi, *Indian J. Phys*. 2009, **83**, 493.

20 A. Weill, "*The Spin Coating Process Mechanism*", Springer Proceedings in Physics, 1986, **13**, 51.

21 Y. D. Park, H. S. Lee, Y. J. Choi, D. Kwak, J. H. Cho, S. Lee and K. Cho, *Adv. Funct. Mater*. 2009, **19**, 1200.

22 J. Clark, J.-F. Chang, F. C. Spano, R. H. Friend and C. Silva, *Appl. Phys. Lett.* 2009*,* **94***,* 163306.

23 M. Chang, D. Choi, B. Fu and E. Reichmanis, *ACS Nano*, 2013, **7**, 5402.

24 H. Yang, T. J. Shin, L. Yang, K. Cho, C. Y. Ryu and Z. N. Bao*, Adv. Funct. Mater.* 2005*,* **15**, 671.

25 C. M. Hansen, "*Hansen Solubility Parameters: A user's handbook*, *Second Edition*". Boca Raton, Fla: CRC Press. ISBN 978-0-8493-7248-3.

26 F. MacHui, S. Langner, X. Zhu, S. Abbott and C. J. Brabec, *Sol. Energy Mater. Sol. C,* 2012, **100**, 138.

27 G. H. Lu, L. G. Li and X. N. Yang, *Adv. Mater.* 2007, **19**, 3594.

28 G. Ridolfi, L. Favaretto, G. Barbarella, P. Samori and N. Camaionì, *J. Mater. Chem.* 2005, **15**, 1704.

29 D. H. Kim, Y. Jang, Y. D. Park and K. Cho, *Langmuir* 2005, **21**, 3203.

30 S. H. Maron, N. Nakajima and I. M. Krieger, *J. Polym. Sci.*, 1959, **37**, 1.

31 A. R. Aiyar, J. Hong, R. Nambiar, D. M. Collard and E. Reichmanis, *Adv. Funct. Mater.* 2011, **21**, 2652.

Journal of Materials Chemistry C Accepted Manuscript

32 K. Armistead and G. Goldbeck-Wood, *Adv. Polym. Sci.* 1992, **100**, 219.

33 H. Hu, K. Zhao, N. Fernandes, P. Boufflet, J. H. Bannock, L. Yu, J. C. de Mello, N. Stingelin, M. Heeney, E. P. Giannelis and A. Amassian, *J. Mater. Chem. C*, 2015, **3**, 7394.

34 K. W. Chou, B. Yan, R. Li, E. Q. Li, K. Zhao, D. H. Anjum, S. Alvarez, R. Gassaway, A. Biocca, S. T. Thoroddsen, A. Hexemer and A. Amassian, *Adv. Mater.* 2013, **25**, 1923.

35 M. Abdelsamie, K. Zhao, M. R. Niazi, K. W. Chou and A. Amassian, *J. Mater. Chem. C*, 2014, **2**, 3373.

36 S. Masubuchi and S. Kazama, *Synth. Met.* 1995*,* **74***,* 151.

37 J. Chang, B. Sun, D. W. Breiby, M. M. Nielsen, T. I. Solling, M. Giles, I. Mcculloch and H. Sirringhaus, *Chem. Mater*. 2004, **16**, 4772.

38 R. J. Kline, M. D. McGehee and M. F. Toney, *Nat. Mater.* 2006, **5**, 222 .

39 R. Jenkins and R. L. Snyder, "*Introduction to X-ray Powder Diffractometry"*, John Wiley & Sons Inc., 1996, p 89-91, ISBN 0-471-51339-3.

40 S. Grigorian, S. Joshi and U. Pietsch, *IOP Conf. Series: Mater. Sci. Eng.* 2010*,* **14**, 012007.

41 S. T. Turner, P. Pingel, R. Steyrleuthner, E. J. W. Crossland, S. Ludwigs and D. Neher, *Adv. Funct. Mater.* 2011, **21**, 4640.

42 Z. Masri, A. Ruseckas, E. V. Emelianova, L. Wang, A. K. Bansal, A. Matheson, H. T. Lemke, M. M. Nielsen, H. Nguyen, O. Coulembier, P. Dubois, D. Beljonne and I. D. W. Samuel, *Adv. Energy Mater.* 2013*,* **3***,* 1445.

43 F. C. Spano, *Chem. Phys.* 2006, **325**, 22.

44 A. Zen, J. Pfaum, S. Hirschmann, W. Zhuang, F. Jaiser, U. Asawapirom, J. P. Rabe, U. Scherf and D. Neher, *Adv. Funct. Mater.* 2004, **14**, 757.

Journal of Materials Chemistry C Accepted Manuscript

.

Journal of Materials Chemistry C Accepted Manuscript

Note and references:

Electronic Supplementary Information (ESI) available. See DOI:

Solvent-dependent self-assembly and ordering in slow-drying drop-cast conjugated polymer films

Kui Zhao,[ab] Xinhong Yu,[b] Ruipeng Li,[c] Aram Amassian[c] and Yanchun Han[b]**

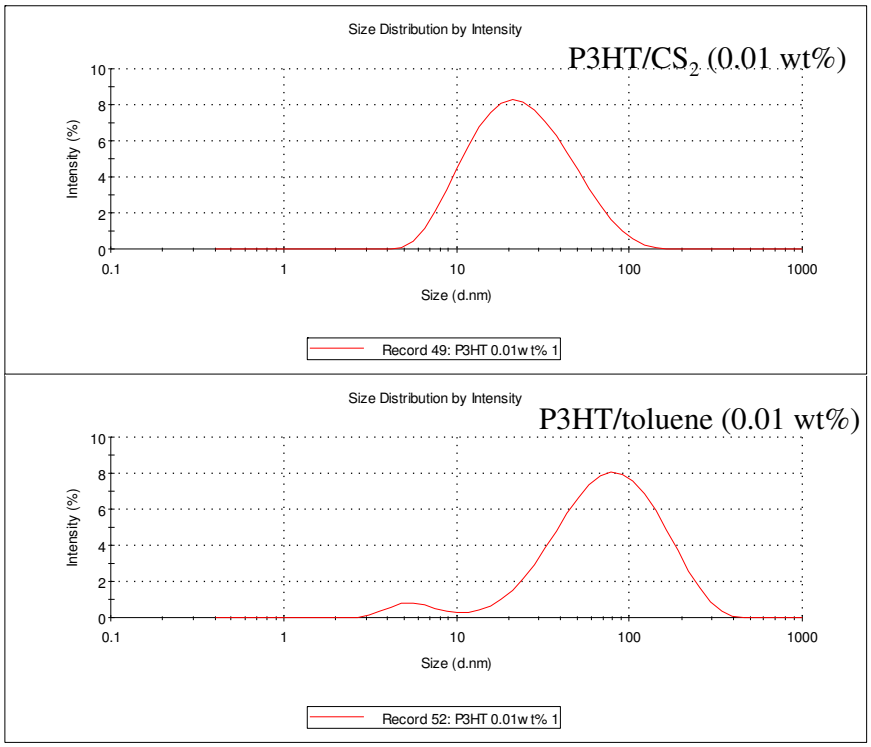

Figure S1. Dynamical light scattering data showing the approximate aggregate size distribution of P3HT solutions in good solvent CS_2 and theta solvent toluene.

Journal of Materials Chemistry C Accepted Manuscript

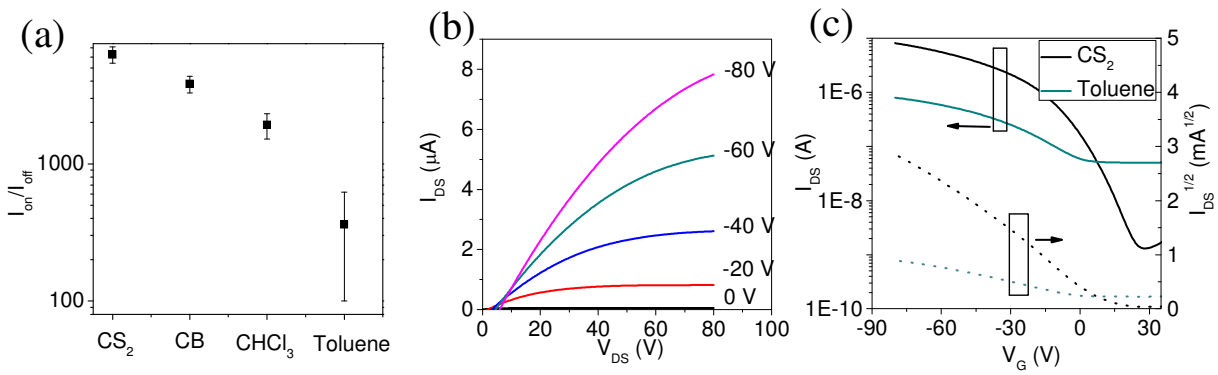

Figure S2. Electrical characteristics in ambient conditions of a representative OTFT with P3HT thin films cast from different solvents. (a) evolution of I_{on}/I_{off} ratio, (b) Output characteristics (I_{DS} *vs.* V_{DS}) with various V_G measured for CS_2-cast film, (c) Transfer characteristics (I_{DS} *vs.* V_G) with a constant V_{DS} for P3HT films cast from good solvent CS_2 and theta solvent toluene.

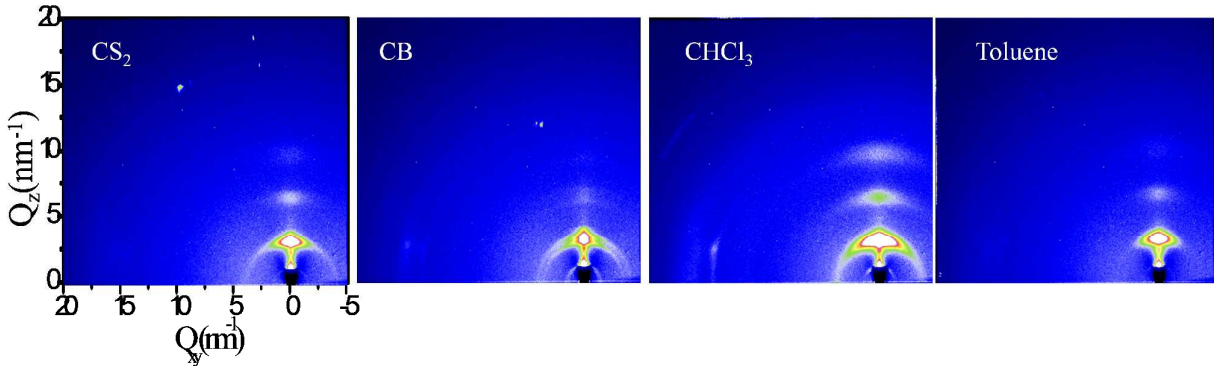

Figure S3. Grazing incidence wide angle X-ray scattering (GIWAXS) of the P3HT films cast from different solvents

Journal of Materials Chemistry C Accepted Manuscript